9. Richter, A. *et al.* Real-space transfer and trapping of carriers into single GaAs quantum wires studied by near-field optical spectroscopy. *Phys. Rev. Lett.* **79,** 2145–2148 (1997).
10. Nötzel, R., Temmyo, J. & Tammamura, T. Tunability of one-dimensional self-faceting on GaAs (311)A surfaces by metalorganic vapor phase epitaxy. *Appl. Phys. Lett.* **64,** 3557–3559 (1994).
11. Nötzel, R., Ledentsov, N., Däweritz, L., Hohenstein, M. & Ploog, K. Direct synthesis of corrugated superlattices on non-(100)-oriented surfaces. *Phys. Rev. Lett.* **67,** 3812–3815 (1991).
12. Okada, Y., Fujita, T. & Kawabe, M. Growth modes in atomic hydrogen assisted molecular beam epitaxy of GaAs. *Appl. Phys. Lett.* **67,** 676–678 (1995).
13. Okada, Y. & Harris, J. S. Jr Basic analysis of atomic-scale growth mechanisms for molecular beam epitaxy of GaAs using atomic hydrogen as a surfactant. *J. Vac. Sci. Technol. B* **14,** 1725–1728 (1996).
14. Miyamoto, Y. & Nonoyama, S. First principles calculation of molecular- and atomic hydrogen reactions on As-terminated GaAs (100) surfaces. *Phys. Rev. B* **46,** 6915–6921 (1992).
15. Gossmann, H. J., Sinden, F. W. & Feldman, L. C. Evolution of terrace size distributions during thin-film growth by step mediated epitaxy. *J. Appl. Phys.* **67,** 745–752 (1990).

Acknowledgements. We thank E. Wiebicke for preparing the patterned substrates. Part of this work was supported by the Bundesministerium für Bildung, Wissenschaft, Forschung und Technologie.

Correspondence and requests for material should be addressed to R.N. (e-mail: notzel@pdi-berlin.de).

Atmospheric CO_2 concentration and millennial-scale climate change during the last glacial period

B. Stauffer*, T. Blunier*, A. Dällenbach*, A. Indermühle*, J. Schwander*, T. F. Stocker*, J. Tschumi*, J. Chappellaz†, D. Raynaud†, C. U. Hammer‡ & H. B. Clausen‡

** Climate and Environmental Physics, Physics Institute, University of Bern, Sidlerstrasse 5, CH-3012 Bern, Switzerland*
† CNRS Laboratoire de Glaciologie (LGGE), BP 96, 38402 St Martin d'Hères Cedex, Grenoble, France
‡ Department of Geophysics, University of Copenhagen, Juliane Maries Vej 30, 2100 Copenhagen O, Denmark

The analysis of air bubbles trapped in polar ice has permitted the reconstruction of past atmospheric concentrations of CO_2 over various timescales, and revealed that large climate changes over tens of thousands of years are generally accompanied by changes in atmospheric CO_2 concentrations[1]. But the extent to which such covariations occur for fast, millennial-scale climate shifts, such as the Dansgaard–Oeschger events recorded in Greenland ice cores during the last glacial period[2], is unresolved; CO_2 data from Greenland[3] and Antarctic[4] ice cores have been conflicting in this regard. More recent work suggests that Antarctic ice should provide a more reliable CO_2 record, as the higher dust[5] content of Greenland ice can give rise to artefacts[1,6,7]. To compare the rapid climate changes recorded in the Greenland ice with the global trends in atmospheric CO_2 concentrations as recorded in the Antarctic ice, an accurate common timescale is needed. Here we provide such a timescale for the last glacial period using the records of global atmospheric methane concentrations from both Greenland and Antarctic ice. We find that the atmospheric concentration of CO_2 generally varied little with Dansgaard–Oeschger events (<10 parts per million by volume, p.p.m.v.) but varied significantly with Heinrich iceberg-discharge events (~20 p.p.m.v.), especially those starting with a long-lasting Dansgaard–Oeschger event.

The $\delta^{18}O$ record of the GRIP ice core[8] confirmed fast and drastic climate variations during the last glacial, so-called Dansgaard-Oeschger events[2,8]. Over Greenland, rapid warmings of several degrees centigrade took place in a few decades, and were followed by a slower cooling and return to full glacial conditions. All but one of the Dansgaard–Oeschger events have a concomitant in ice-rafting debris recorded in sediment cores from the North Atlantic[9]. Simulations with ocean circulation models suggest that the fresh-water input resulting from iceberg discharge has the potential to alter the North Atlantic Deep Water (NADW) formation[10–12]. The effect of changes of the deep ocean circulation and of the marine biogeochemistry on the atmospheric CO_2 concentrations is an important open question.

Measurements of the CO_2 concentration in the air bubbles entrapped in ice cores from Greenland revealed large CO_2 variations, with levels of ~200 p.p.m.v. during the cold phases and ~250 p.p.m.v. during the mild phases of Dansgaard–Oeschger events[3]. Detailed measurements on the Byrd ice core (from Antarctica) did not show variations of this magnitude[4,13]. It is now believed that the high CO_2 concentrations during mild phases in the Greenland ice cores do not represent the atmospheric concentration but are caused by an acid-carbonate reaction or by oxidation of organic material in the ice[6,7]. Ice cores from Antarctica are less affected by such reactions[1,6,7].

Because the atmospheric CO_2 concentration can only be detected reliably in Antarctic ice, ice cores from both hemispheres are needed to investigate a possible correlation between fast climate changes in the Northern Hemisphere and the atmospheric CO_2 concentration. This requires precise synchronization of the age scales from Greenland and Antarctic ice cores. Sowers *et al.*[14] showed that a synchronization of ice cores can be done using the global $\delta^{18}O$ signal of O_2. Another powerful tool is now available to synchronize the GRIP ice core from Greenland and the Byrd ice core from Antarctica; this tool is based on high-resolution methane records[15]. The accuracy of the synchronization is a factor of ten better with methane owing to the fast variations of the atmospheric CH_4 concentration. The variations are global, because the atmospheric residence time of CH_4 is

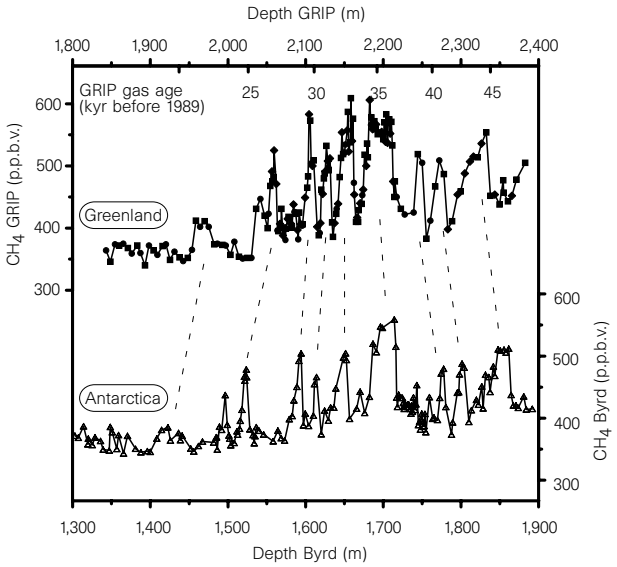

Figure 1 Methane concentrations measured on the GRIP and Byrd ice cores. Solid line with open triangles, Byrd station; solid line with filled symbols, GRIP (circles, published data[17]; squares, new data from the Physics Institute, University of Bern; diamonds, new data from the CNRS Laboratoire de Glaciologie, Grenoble). In both laboratories a melting–refreezing method was used to extract the gas from the ice[16,17]. An ice sample was melted under vacuum in a glass container and then refrozen from the bottom. The extraction efficiency is close to 100%. The extracted air was then expanded into a sample loop and injected into a gas chromatograph equipped with a thermal conductivity detector (TCD) and a flame ionization detector (FID). The dashed lines denote peak values which are considered to characterize synchronous events. This identification is based on a Monte Carlo method maximizing the correlation between the two CH_4 records ($r^2 = 0.76$). The absolute timescale in kyr before 1989 (top) applies only to the GRIP record[8,19].

ten times larger than the interhemispheric exchange time[16]. Nevertheless, the interhemispheric CH_4 difference of ~5% may change slightly over time owing to changes in the latitudinal distribution of sources and sinks, as demonstrated for the Holocene period[16]. The methane records measured along the GRIP and the Byrd ice core show distinct variations, with a very similar pattern in the period 20–45 kyr before present, BP (Fig. 1). The covariance between CH_4 data from different sites confirms that the variations are of atmospheric origin. The GRIP methane variations parallel the Dansgaard–Oeschger events. During cold phases the concentration of methane is ~350 p.p.b.v. and during mild phases between 450 and 550 p.p.b.v. (ref. 17).

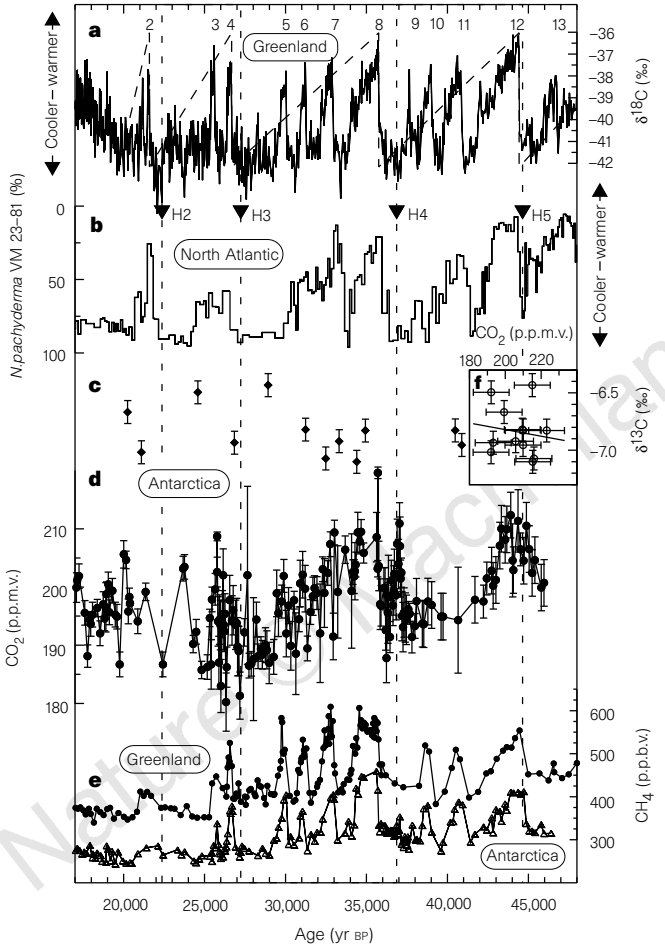

Figure 2 Comparison of CO_2 variations and climate changes. **a**, $\delta^{18}O$ values for the GRIP ice core[8] together with Bond long-term cooling cycles, schematically shown as saw-tooth[20]. **b**, *N. Pachyderma* record from the deep sea core V23-81 (54° 15′ N, 16° 50′ W) as a proxy for sea surface temperature. Filled triangles show Heinrich events (ice-rafting events originating from the Hudson Strait)[9,20]. **c**, $\delta^{13}C$ values measured on CO_2 extracted from Byrd ice samples[26]. **d**, Byrd ice-core CO_2 values[4] on the adjusted timescale. It is remarkable that the CO_2 concentration between Heinrich events 2 and 3, which shows only two narrow mild phases and a *N. pachyderma* abundance above 50%, remains smaller than between Heinrich events 3–4 and 4–5, where broad mild phases and *N. pachyderma* abundance below 50% are observed. **e**, Methane records of the GRIP and Byrd ice cores as in Fig. 1 but now plotted on the adjusted common timescale. Byrd values were lowered by 100 p.p.b.v. for better readability. **f**, $\delta^{13}C$ values plotted against CO_2 values measured on the same ice samples. The CO_2 measurements have been done volumetrically[26] which explains a higher uncertainty ($\sigma = \pm 10$ p.p.m.v.) compared to the results presented in **d**. The linear regression line shows an anticorrelation. A Monte Carlo simulation confirmed a very weak anticorrelation between $\delta^{13}C$ and CO_2 values. **a** and **b** are sections of Fig. 3 of Bond *et al.*[9,20].

Based on the fast CH_4 oscillations, a synchronization of the CH_4 signals is possible with an accuracy of about two centuries[15] which is the typical timescale for methane increases at the beginning of a mild event. As timescale, we selected the one of the GRIP ice core[8,18] for easier reference, but our conclusions do not depend on this choice. Because the occlusion of gases takes place typically at 70 m below the snow surface, the air in the bubbles is younger than the surrounding ice[19]. The age difference for GRIP varies between 350 and 1,290 yr with an uncertainty of ±300 yr over the time range 47–17 kyr BP (ref. 19). The CH_4 records of both cores were matched using a Monte Carlo method, looking for maximum correlation between the two records[19]. Table 1 gives the depth as a function of the gas age for the GRIP and the Byrd ice core.

In Fig. 2, the Byrd CH_4 and CO_2 records with the adjusted Byrd timescale are shown, together with CH_4 and $\delta^{18}O$ records from the GRIP ice core. The age difference between ice and enclosed air is irrelevant for the comparison of only CH_4 and CO_2 records between two cores, and the accuracy of this synchronization is estimated to be ~200 yr. For the comparison of gas records with ice records, for example, the Byrd CO_2 record with the GRIP $\delta^{18}O$ record, the age difference between gases and ice is important. The uncertainty in this special case is only ~360 yr, because the age difference is well known for the GRIP ice core owing to a reliable timescale and precisely determined accumulation rates. A synchronization of the $\delta^{18}O$ records of the two cores could be achieved as soon as the age difference between gases and ice is determined for the Byrd core with a similar accuracy as for the GRIP core.

Together with the GRIP $\delta^{18}O$ record, the abundance of *Neogloboquadrina pachyderma* (s.) from the North Atlantic core V23-81 (refs 9, 20) (which is a proxy for sea surface temperature (SST)), and the position of the Heinrich layers are indicated in Fig. 2. The adjustment of the marine timescale has been done as in the original publication by Bond *et al.*[20].

The Byrd CO_2 concentration varies between about 180 and 210 p.p.m.v. during 47–17 kyr BP. We can therefore definitely exclude atmospheric CO_2 concentration variations parallel to Dansgaard–Oeschger events of the order of 50 p.p.m.v. as suggested by the measurements on Greenland ice cores[3]. The amplitudes of

Table 1 Depth versus age for ice-core samples

Gas age (yr BP)	GRIP depth (m)	Byrd depth (m)
17,000	1,854	1,284
18,000	1,889	1,317
19,000	1,916	1,350
20,000	1,937	1,383
21,000	1,958	1,410
22,000	1,979	1,421
23,000	1,994	1,432
24,000	2,010	1,446
25,000	2,026	1,472
26,000	2,046	1,504
27,000	2,068	1,530
28,000	2,080	1,552
29,000	2,093	1,573
30,000	2,112	1,594
31,000	2,125	1,613
32,000	2,140	1,633
33,000	2,162	1,653
34,000	2,173	1,673
35,000	2,192	1,702
36,000	2,216	1,722
37,000	2,225	1,742
38,000	2,237	1,763
39,000	2,253	1,780
40,000	2,263	1,793
41,000	2,281	1,805
42,000	2,290	1,817
43,000	2,305	1,832
44,000	2,323	1,850
45,000	2,338	1,867
46,000	2,347	1,885

Depths are given in m below surface. The uncertainty of the gas age relative to the age scale of the ice[18] is ~300 yr for the GRIP core and ~360 yr for the Byrd core.

methane variations, tracking all Dansgaard–Oeschger events, are of the same magnitude in both the GRIP and the Byrd ice cores. This also rules out the possibility that atmospheric CO_2 concentration changes with similar frequencies and similar durations would be recorded in attenuated form in the Byrd core because of its lower accumulation rate (which causes a broader age distribution of the air enclosed in bubbles at a given depth). However, CO_2 variations with a smaller amplitude parallel to Dansgaard–Oeschger events cannot be excluded with the available results. For example, there is a direct correlation of $r = 0.55$ between CO_2 concentrations and $\delta^{18}O$ (individual Dansgaard–Oeschger events) for the time interval 26–45 kyr BP, including H3–H5. On the other hand, we suggest, based on Fig. 2d, that atmospheric CO_2 variations and Bond cooling cycles between successive Heinrich events are linked slightly better; for the same time interval of 26–45 kyr BP (two Bond cycles) the correlation between CO_2 and Bond cycles (saw-tooth in Fig. 2a) is 0.57. The higher values of CO_2 correlate quite well with the two Bond cycles following the principal events H5 and H4. These two cycles are also distinct in that their initial mild phases are pronounced and last for more than 2 kyr (following H4) and more than 3 kyr (following H5) rather than just 1 kyr typical for all other Dansgaard–Oeschger events. In contrast, the Bond cycle starting after H3 contains only two very short Dansgaard–Oeschger events that are similar to the later events around 31 and 38 kyr BP. None of these Dansgaard–Oeschger events is reflected in clear atmospheric CO_2 variations, suggesting that they are too short, or too localized in space, to have a net effect on the atmospheric CO_2 concentration. The cycle following H2 is influenced already by the transition from the glacial to the Holocene epoch.

Before discussing the information that this signal carries about the coupled climate–carbon cycle system, the possibility of *in situ* production of CO_2 must be addressed. The impurities of Antarctic ice of the Holocene are generally very low, and carbonate concentrations were found[21] to be below the detection limit of 0.1 $\mu mol\,l^{-1}$. For the glacial period the situation is less clear. Byrd glacial ice is in many respects comparable to GRIP Holocene ice (acidity[22], dust concentration[5], carbonate level[21]). In the latter core, an acid-carbonate reaction or oxidation of organic material takes place, causing a scatter of CO_2 measurements from neighbouring samples ($\sigma \approx 15$ p.p.m.v.) that is much larger than the analytical uncertainty[23] ($\approx \pm 3$ p.p.m.v.). We conclude from the lower scatter in the CO_2 measurements from Byrd glacial ice ($\sigma \approx 4$ p.p.m.v.) that chemical reactions are less important in the Byrd ice core, and that the Byrd CO_2 record probably represents variations of the atmospheric CO_2 concentration. The Vostok (Antarctica) CO_2 record[24] is in agreement with the Byrd results[4], but lacks sufficient resolution for comparison with the present data. Byrd data from the early Holocene agree in magnitude with detailed measurements from D47 (Antarctica) in a short overlapping period (7–6 kyr BP)[25]. However, Byrd Holocene data show more scatter, due, we believe, to bad core quality in the corresponding depth interval. Detailed CO_2 records should become available from analyses of the already recovered ice cores from Taylor Dome (by the United States) and Dome Fuji (by Japan) and from the cores to be recovered by EPICA (European Project for Ice Coring in Antarctica) at Dome Concordia and Dronning Maud Land. We hope that these records will provide an extension of the investigations to older ages and additional cycles and so confirm the present results. However, a correlation alone does not necessarily exclude the possibility of an artefact. Greenland CO_2 records from Dye 3, Camp Century and Summit all show CO_2 variations of the order of 50 p.p.m.v. parallel to Dansgaard–Oeschger events, although none of these variations are atmospheric. Only a combination of detailed CO_2 and chemical analyses of the various cores will finally allow us decide whether the CO_2 record shown in Fig. 2 indeed represents atmospheric CO_2 variations.

Although sparse, the $\delta^{13}C$ record of CO_2 (ref. 26) carries some information about the origin of the CO_2 concentration variations. $\delta^{13}C$ seems to be rather in anticorrelation than in correlation with the CO_2 concentration. The assumption of an anticorrelation is supported by measurements on an ice core from the South Yamato mountains (Antarctica)[27]. The *N. pachyderma* record from the North Atlantic indicates that the long-term SST and CO_2 concentration are fairly well correlated. Lower SST correspond to lower CO_2 concentrations. Indeed, a lowered surface temperature leads to an increased CO_2 uptake due to the higher solubility but this leads as well to a lowered $\delta^{13}C$ value. Because this is not observed in $\delta^{13}C$, CO_2 uptake by lowered SST is probably not the main reason for the lowering of the CO_2 concentration. Increased activity of the biological pump or increased terrestrial biomass lead to a depletion of the atmospheric CO_2 content parallel to an increase in the $\delta^{13}C$ ratio[28]. They are therefore both candidates for explaining the observed CO_2 and $\delta^{13}C$ variations. The biological pump is the more likely, because one would not expect a higher terrestrial biomass during cold phases. Additional $\delta^{13}C$ measurements and simulations with dynamical climate models including the carbon cycle[29] will be needed to quantify the contributions of the different mechanisms.

The greatest concentrations of atmospheric CO_2 are generally associated with the strongest (in amplitude and duration) Dansgaard–Oeschger cycles following a Heinrich event. Such cycles also represent fast and abrupt changes in the Northern Hemisphere temperature, but there seem to be no significant CO_2 increases parallel to short Dansgaard–Oeschger cycles. We suggest that either the dynamics of these cycles are distinctly different from that of Heinrich events or that the response time for CO_2 to reach a new equilibrium is too long compared to the timescale of these Dansgaard–Oeschger cycles.

Determination of the relation between climate and global CO_2 concentration remains a challenge. Further high-precision $\delta^{13}C$ and CO_2 measurements, along with climate proxies on a synchronized timescale, are needed to understand the past CO_2 cycle. Such measurements would also be useful in the prediction of future climate change. □

Received 17 February; accepted 24 November 1997.

1. Raynaud, D. *et al.* The ice record of greenhouse gases. *Science* **259,** 926–933 (1993).
2. Oeschger, H. *et al.* in *Climate Processes and Climate Sensitivity* (eds Hansen, J. E. & Takahashi, T.) 299–306 (Vol. 29, Geophys. Monogr Ser., Am Geophys. Union, Washington DC, 1984).
3. Stauffer, B., Hofer, H., Oeschger, H., Schwander, J. & Siegenthaler, U. Atmospheric CO_2 concentration during the last glaciation. *Ann. Glaciol.* **5,** 160–164 (1984).
4. Neftel, A., Oeschger, H., Staffelbach, T. & Stauffer, B. CO_2 record in the Byrd ice core 50,000–5,000 years BP. *Nature* **331,** 609–611 (1988).
5. Thompson, L. G. in *Proc. Isotopes and Impurities in Snow and Ice*, Grenoble Aug./Sept. 1975, 351–363 (Publication 118, Int. Assoc. Hydrological Sciences, IAHS-AISH, 1975).
6. Delmas, R. A. A natural artefact in Greenland ice-core CO_2 measurements. *Tellus B* **45,** 391–396 (1993).
7. Anklin, M. *et al.* CO_2 record between 40 and 8 kyr BP from the GRIP ice core. *J. Geophys. Res.* **102,** 26539–26545 (1997).
8. Dansgaard, W. *et al.* Evidence for general instability of past climate from a 250-kyr ice-core record. *Nature* **364,** 218–220 (1993).
9. Bond, G. C. & Lotti, R. Iceberg discharges into the North Atlantic on millennial time scales during the last deglaciation. *Science* **267,** 1005–1010 (1995).
10. Maier-Reimer, E. & Mikolajewicz, U. *Experiments with an OGCM on the Cause of the Younger Dryas* (Tech. Rep. 39, Max-Planck-Inst. für Meteorol, Hamburg, 1989).
11. Stocker, T. F. & Wright, D. G. Rapid transitions of the ocean's deep circulation induced by changes in surface water fluxes. *Nature* **351,** 729–732 (1991).
12. Wright, D. G. & Stocker, T. F. in *Ice in the Climate System* (ed. Peltier, W. R.) 395–416 (NATO ASI Ser. I, 12, Springer, Berlin, 1993).
13. Oeschger, H., Neftel, A., Staffelbach, T. & Stauffer, B. The dilemma of the rapid variations in CO_2 in Greenland ice cores. *Ann. Glaciol.* **10,** 215–216 (1988).
14. Sowers, T. & Bender, M. Climate records covering the last deglaciation. *Science* **269,** 210–214 (1995).
15. Blunier, T. *et al.* Timing of the Antarctic Cold Reversal and the atmospheric CO_2 increase with respect to the Younger Dryas event. *Geophys. Res. Lett.* **24,** 2683–2686 (1997).
16. Chappellaz, J. *et al.* Changes in the atmospheric CH_4 gradient between Greenland and Antarctica during the Holocene. *J. Geophys. Res.* **102,** 15987–15999 (1997).
17. Chappellaz, J. *et al.* Synchronous changes in atmospheric CH_4 and Greenland climate between 40 and 8 kyr BP. *Nature* **366,** 443–445 (1993).
18. Johnsen, S. J., Dahl-Jensen, D., Dansgaard, W. & Gundestrup, N. Greenland paleotemperatures derived from GRIP bore hole temperature and ice core isotope profiles. *Tellus B* **47,** 624–629 (1995).
19. Schwander, J. *et al.* Age scale of the air in the Summit ice: Implication for glacial-interglacial temperature change. *J. Geophys. Res.* **102,** 19483–19494 (1997).
20. Bond, G. *et al.* Correlations between climate records from North Atlantic sediments and Greenland ice. *Nature* **365,** 143–147 (1993).
21. Fuhrer, A. *Ein System zur Messung des totalen Karbonatgehaltes polarer Eisproben* Thesis, Univ. Bern (1995).
22. Hammer, C. U., Clausen, H. B. & Langway, C. C. Jr Electrical conductivity method (ECM) stratigraphic dating of th Byrd Station ice core, Antarctica. *Ann. Glaciol.* **20,** 115–120 (1994).

23. Anklin, M. J. *Kohlenstoffdioxid Bestimmungen in Luftproben aus einem neuen Tiefbohrkern von Summit (Grönland)* Thesis, Univ. Bern (1994).
24. Barnola, J.-M., Pimienta, P., Raynaud, D. & Korotkevich, Y. S. CO_2-climate relationship as deduced from the Vostok ice core: A re-examination based on new measurements and on a re-evaluation of the air dating. *Tellus* **43,** 83–90 (1991).
25. Barnola, J.-M., Jeanjean, E. & Raynaud, D. Holocene atmospheric CO_2 evolution as deduced from an Antarctic ice core. *Eos* **77,** 151 (1996).
26. Leuenberger, M., Siegenthaler, U. & Langway, C. C. Carbon isotope composition of atmospheric CO_2 during the last ice age from an Antarctic ice core. *Nature* **357,** 488–490 (1992).
27. Machida, T. *et al.* Variations of the CO_2, CH_4 and N_2O concentrations and $\delta^{13}C$ of CO_2 in the glacial period deduced from an Antarctic ice core, south Yamato. *Proc. NIPR Symp. Polar Meteorol. Glaciol.* **10,** 55–65 (1996).
28. Keir, R. S. On the Late Pleistocene ocean geochemistry and circulation. *Paleoceanography* **3,** 413–445 (1988).
29. Marchal, O., Stocker, T. F. & Joos, F. Impact of oceanic reorganisations and the marine carbon cycle and atmospheric CO_2. *Paleoceanography* (submitted).

Acknowledgements. We thank M. Leuenberger and J.-M. Barnola for discussions, and F. Finet for measuring additional CH_4 samples at LGGE. This work, as part of the Greenland Ice Core Project (GRIP), was supported by the University of Bern, the Swiss National Science Foundation, the Federal Department of Energy (BEW), the Schwerpunktprogramm Umwelt (SPPU) of the Swiss National Science Foundation, the EC programme "Environment and Climate 1994–1998", the Fondation de France and the Programme National de Dynamique du Climat of CNRS.

Correspondence and requests for materials should be addressed to B.S. (e-mail: stauffer@climate.unibe.ch).

Influence of sea-salt on aerosol radiative properties in the Southern Ocean marine boundary layer

D. M. Murphy*, J. R. Anderson†, P. K. Quinn‡, L. M. McInnes§, F. J. Brechtel‖, S. M. Kreidenweis‖, A. M. Middlebrook*¶, M. Pósfai#, D. S. Thomson*¶ & P. R. Buseck†#

* *Aeronomy Laboratory, National Oceanic and Atmospheric Administration, Boulder, Colorado 80303, USA*
† *Department of Chemistry and Biochemistry, Arizona State University, Tempe, Arizona 85287, USA*
‡ *Pacific Marine Environment Laboratory, National Oceanic and Atmospheric Administration, Seattle, Washington 98115, USA*
§ *Climate Monitoring and Diagnostics Laboratory, National Oceanic and Atmospheric Administration, Boulder, Colorado 80303, USA*
‖ *Department of Atmospheric Science, Colorado State University, Fort Collins, Colorado 80523, USA*
¶ *Cooperative Institute for Research in the Environmental Sciences, University of Colorado, Boulder, Colorado 80309, USA*
# *Department of Geology, Arizona State University, Tempe, Arizona 85287, USA*

There has been considerable debate about the relative importance of sea-salt and sulphate from non-sea-salt sources in determining aerosol radiative effects in the marine boundary layer. In the marine boundary layer, the most numerous aerosols are volatile sulphate particles smaller than about 0.08 μm (ref. 1) and most of the aerosol mass is in a few sea-salt particles larger than 1 μm. Yet intermediate-size aerosols between about 0.08 and 1 μm diameter are the most relevant to the radiative forcing of climate because they efficiently scatter solar radiation and also serve as cloud nuclei[2]. Indeed, Charlson *et al.*[3] hypothesized that oceanic production of sulphate aerosols from the oxidation of dimethyl sulphide could be a powerful feedback in the climate system. It is generally assumed that marine aerosols smaller than about 1 μm are non-sea-salt sulphate, but a recent review cites indirect evidence that many aerosols in the sub-micrometre range contain at least some sea-salt[4,5]. Here we present direct observational evidence from a remote Southern Ocean region that almost all aerosols larger than 0.13 μm in the marine boundary layer contained sea-salt. These sea-salt aerosols had important radiative effects: they were responsible for the majority of aerosol-scattered light, and comprised a significant fraction of the inferred cloud nuclei.

The first Aerosol Characterization Experiment (ACE-1) included complementary techniques to assess the chemical and radiative properties of aerosols in the marine boundary layer (MBL). The composition of aerosols was measured by electron microscopy and mass spectrometry of single particles, aerosol volatility and bulk analysis of size-segregated aerosol samples. At Cape Grim, Tasmania (41° S, 145° E), the elemental composition of individual particles collected on filters and grids was determined using automated scanning and manual transmission electron microscopy (SEM,

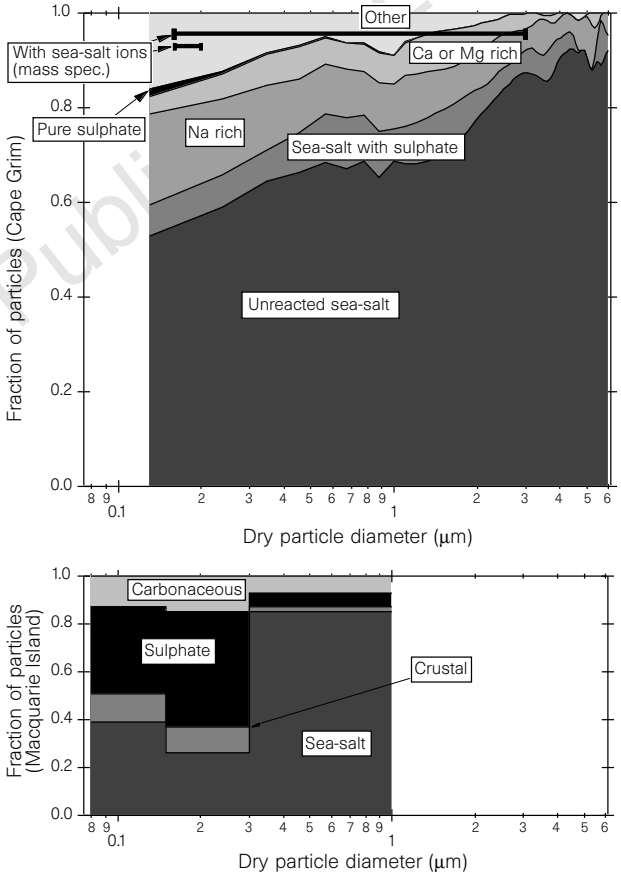

Figure 1 The chemical composition of particles at Cape Grim and Macquarie Island as a function of their diameter. Top, composition at Cape Grim from automated SEM analysis (filled areas, $n = 19{,}640$). Also shown are the fraction of particles analysed by mass spectrometry that contained detectable sea-salt ions ($n = 5{,}240$). The two bars are for samples taken with or without a mobility analyser to select only a limited size range for analysis. Bottom, composition at Macquarie Island from manual TEM analysis ($n = 4$ samples, 300 particles). SEM data at Cape Grim were classified using cluster analysis, then the clusters were grouped into the categories shown here 'Unreacted sea-salt' includes particles with elemental compositions very close to natural sea-salt. The 'other' category includes particles that contained only light elements, salt particles with compositions far from sea-salt, and unusual particles such as soot or metals. For samples from Macquarie Island, sea-salt-containing particles were defined as those containing appropriate quantities of Na, Mg, Ca, K and variable quantities of S, with or without measurable quantities of Cl. In the mass spectra, particles containing sea-salt were identified by the presence of Cl in the negative ions and Na or K in the positive ions. The mass spectrometer measured a higher fraction of sea-salt-containing particles because it is very sensitive to Cl and Na. However, as typified in Fig. 2, most of the mass spectra showed a substantial fraction of sea-salt.